He Qing (Orcid ID: 0000-0002-3401-5898)
Dieppois Bastien (Orcid ID: 0000-0001-7052-1483)
Yetemen Omer (Orcid ID: 0000-0003-1593-3519)
Schoppach Remy (Orcid ID: 0000-0002-9500-7007)
Çağlar Ferat (Orcid ID: 0000-0002-2584-2883)

Impact of the North-Sea Caspian pattern on Meteorological drought and Vegetation Response over diverging environmental systems in western Eurasia

Qing He[1], Bolin Xu[1], Bastien Dieppois[2, 3], Ömer Yetemen[4], Omer Lutfi Sen[4], Julian Klaus[5], Remy Schoppach[6], Ferat Çağlar[4], Ping Yu Fan[1], Liang Chen[7], Luminita Danaila[8], Nicolas Massei[8], and Kwok Pan Chun[1, 9]*

[1] Department of Geography, Hong Kong Baptist University, Hong Kong SAR, China

[2] Centre for Agroecology, Water and Resilience, Coventry University, UK

[3] Department of Oceanography, University of Cape Town, South Africa

[4] Eurasia Institute of Earth Sciences, Istanbul Technical University, Istanbul, Turkey

[5] Department of Geography, University of Bonn, Germany

[6] Catchment and Eco-hydrology Research Group, Department of Environmental Research and Innovation, Luxembourg Institute of Science and Technology, Esch/Alzette, Luxembourg

[7] Key Laboratory of Regional Climate Environment for Temperate East Asia, Institute of Atmospheric Physics, Chinese Academy of Sciences, Beijing, China

[8] M2C Laboratory, The University of Rouen Normandy, France

[9] Department of Geography and Environmental Management, University of the West of England, Bristol, UK

This article has been accepted for publication and undergone full peer review but has not been through the copyediting, typesetting, pagination and proofreading process which may lead to differences between this version and the Version of Record. Please cite this article as doi: 10.1002/eco.2446

Abstract

Emerging drought stress on vegetation over western Eurasia is linked to varying teleconnection patterns. The North-Sea Caspian pattern (NCP) is a relatively less studied Eurasian teleconnection pattern which has a role on drought conditions and the consequence of changing conditions on vegetation. Between 1981 and 2015, we found that the Standardized Precipitation Index (SPI) and the Normalized Difference Vegetation Index (NDVI) have different trend patterns over various parts of western Eurasia. Specifically, the vegetation greenness is linked with wetter conditions over Scandinavia, and vegetation cover decreases over a drying central Asia. However, in western Russia and France, there are paradoxically becoming greener under drier conditions. Using the Budyko framework such paradoxical patterns are found in energy-limited environmental systems, where vegetation growth is primarily promoted by warmer temperatures.

While most studies focused on the impacts of the North Atlantic Oscillation (NAO), we test whether the NCP explains better the variability of meteorological drought and vegetation response over western Eurasia. We hypothesised that the positive phases of the NCP are correlated to high pressure anomalies over the North Sea, which can be associated with weakening onshore moisture advection, leading to warmer and dryness conditions. These conditions are driving vegetation greening, as western Eurasia is mainly energy-limited. However, we show that as the climate is warming along with the teleconnection impacts, the future ecosystem over western Eurasia will be transferred from energy-limited to water-limited systems. This suggests that the observed vegetation greening over past three decades is unlikely to sustain in the future.

Keywords

Western Eurasia, North Sea-Caspian Pattern (NCP), drought conditions, Standardized Precipitation Index (SPI), Normalized Difference Vegetation Index (NDVI), Budyko framework

Highlights

- Trends show a vegetation greening (NDVI) in most western Eurasia but increasingly drying conditions (less precipitation and higher temperature)
- NCP is better than NAO for explaining drought variability based on evaporative indices in western Eurasia
- Regional oscillations between energy- and water- limited conditions are related to NCP
- Vegetation over western Eurasia is likely to suffer from increasing water stress

Significance Statement

Meteorological droughts affect vegetation cover differentially across western Eurasia depending on local water and energy availability. Droughts hinder vegetation development in water-limited areas, but promote vegetation growth in energy-limited areas due to rising temperatures. The teleconnections that influence precipitation and temperature patterns are linked to these patterns of vegetation responses. The North Sea-Caspian Pattern (NCP) explains more variance between meteorological drought and vegetation response over

western Eurasia than the North Atlantic Oscillation (NAO), a commonly studied teleconnection pattern. The observed vegetation greening over the last three decades is unlikely to persist, given the effects of rising temperatures and NCP changes.

1 Introduction

Vegetation growth over western Eurasia has been linked with large-scale teleconnections, local hydrological conditions and temperature increase from the early 1980s (Gouveia, Trigo, DaCamara, Libonati, & Pereira, 2008; Olafsson & Rousta, 2021). Hydroclimate conditions over western Eurasia are shown to be modulated by several teleconnection pattern including the North Atlantic Oscillation (NAO; Deser, Hurrell, & Phillips, 2017; Iles & Hegerl, 2017; Tsanis & Tapoglou, 2019), Atlantic Oscillation (AO; Báez et al., 2014; D. Y. Lee, Lin, & Petersen, 2020), East Atlantic (EA; Ionita, 2014; Toreti, Desiato, Fioravanti, & Perconti, 2010; Tošić & Putniković, 2021; Ulbrich et al., 2012), El Nino Southern Oscillation (ENSO; R. W. Lee, Woolnough, Charlton-Perez, & Vitart, 2019; Mezzina, García-Serrano, Bladé, & Kucharski, 2020), and South Asian monsoon (SAM; Alpert et al., 2006). Despite well documented teleconnections between these different modes of climate variability and hydroclimate conditions in previous studies (Lledó, Cionni, Torralba, Bretonnière, & Samsó, 2020; Rousi, Rust, Ulbrich, & Anagnostopoulou, 2020; Rust, Holman, Corstanje, Bloomfield, & Cuthbert, 2018), the impact of the North Sea-Caspian Pattern (NCP), remains largely unexplored. The NCP is an upper-level atmospheric teleconnection with centres of active variability over the North Sea and the Caspian Sea regions. These seas are regional water bodies, which affect the common locations of local pressure systems due to seasonal circulation variations driven by temperature gradients caused by differences of thermal capacity between land and water (Dippner, Möller, & Hänninen, 2012; Sibley, Cox, & Titley, 2015). To date, NCP effects on temperature and precipitation have been studied mainly for the East Mediterranean and its surrounding regions (Kutiel, Maheras, Türkeş, & Paz, 2002; Kutiel & Türkeş, 2005; Sezen & Partal, 2019). However, given that the NCP centres of action are farther north, it might strongly impact precipitation patterns, hence drought occurrence and vegetation conditions over the entire Eurasia (Brunetti & Kutiel, 2011; Çağlar, Yetemen, Pan Chun, & Lutfi Sen, 2021).

In recent decades, western Eurasia has experienced several severe drought events, notably in 2002, 2003, 2015 and 2018, due to large-scale climate variability (Buras & Rammig, 2020; Ionita et al., 2017; Rimkus, Stonevicius, Kilpys, MacIulyte, & Valiukas, 2017). These droughts strongly impacted agricultural activities and ecological services (Changnon, 2003; Murnane, 2004; Parmesan, Root, & Willig, 2000). Vegetation indices serve as a crucial ecohydrological indicator of terrestrial ecosystems and agriculture (Measho et al., 2019; Niu, Kang, Zhang, & Fu, 2019; Sawada, 2018). Detecting and monitoring the onset and early-stage of droughts are therefore of critical significance for predicting the impacts on vegetation conditions and anticipate eco-environmental management actions on a regional scale (Bachmair, Tanguy, Hannaford, & Stahl, 2018; Sutanto, van der Weert, Wanders, & Blauhut, 2019).

Droughts are traditionally quantified by water availability indices, such as Standardized Precipitation Index (SPI) (Cancelliere, Mauro, Bonaccorso, & Rossi, 2007; Livada & Assimakopoulos, 2007; McKee, Doesken, & Kleist, 1993). Given the direct effects of

droughts on vegetation, vegetation indices (van Hateren, Chini, Matgen, & Teuling, 2021), have also been used as drought indicators (Buitink & Swank, 2020; Hu et al., 2019; Sepulcre-Canto, Horion, Singleton, Carrao, & Vogt, 2012; Di Wu, Qu, & Hao, 2015). However, there are various factors that may lead the vegetation to be less affected by the declining water availability due to compensation by warming temperatures (Peng et al., 2011; X. Wang et al., 2017; G. Xu et al., 2014), increasing solar irradiation (Teuling, 2013), and increasing CO_2 fertilization (Lian et al., 2021). According to previous studies, the vegetation responses to drought conditions are divergent for different climate environments, and the similarity and differences in water and vegetation variability needs to be further explored (Denissen, Teuling, Reichstein, & Orth, 2020; Peled, Dutra, Viterbo, & Angert, 2010; van Hateren et al., 2021). To explore the long-term interactions among climate, regional hydrology and vegetation cover, which is related to the water-limited and energy-limited environment, the Budyko framework is applied (Abera, Tamene, Abegaz, & Solomon, 2019; Li, Pan, Cong, Zhang, & Wood, 2013; D. Zhang, Liu, & Bai, 2018).

In Section 2, we introduce the study area, data sources, and methods. In Section 3, we examine the similarity and disparity in meteorological and vegetation variations over western Eurasia. Then, we test whether NCP can be a better contributor than NAO to explain changes in meteorological and vegetation conditions, and describe the mechanisms associated with NCP teleconnections over various environmental systems. In Section 4 and 5, we discuss their wider implications and summarise the main results.

2 Data and methods

2.1 Study area

The study is centred on western Eurasia (i.e. 10°W-70°E and 35°N-72°N; Figure 1). The western part of the study region has an oceanic/maritime climate with temperate summers and mild winters, whereas the central and eastern parts have a continental climate with hot summers and cold winters (Stampoulis & Anagnostou, 2012). Due to different climate zones of western Eurasia, water and vegetation are unevenly distributed. The total amount of precipitation ranges from 600-900 $mm.yr^{-1}$ over the western part to 500 $mm.yr^{-1}$ in the eastern part of western Eurasia (Mikolaskova, 2009). The main vegetation cover types vary from woody savannas and mixed forest in the high latitudes to croplands and grassland in the mid-latitudes (Figure 1).

2.2 Data

2.2.1 Normalized Difference Vegetation Index (NDVI) data

As a proxy of vegetation greenness, the Normalized Difference Vegetation Index (NDVI) is extracted from the NOAA Global Inventory Monitoring and Modeling System (GIMMS), version number 3g.v1 (Cai et al., 2014; Pinzon & Tucker, 2014; Donghai Wu et al., 2014). This dataset provides bi-monthly data (~every 14 days), with a 1/12 degree resolution, between July 1981 and December 2015. In order to validate the GIMMS NDVI datasets, we use the monthly NDVI dataset from the Moderate Resolution Imaging Spectroradiometer (MODIS MOD13C2), which is available at 0.05° resolution (Fensholt & Proud, 2012; Solano, Didan, Jacobson, & Huete, 2010). For comparison, the GIMMS NDVI data were made to be monthly by averaging the two values in each month. We found that both datasets are largely

similar in terms of seasonal and interannual variations (Figure S1).

2.2.2 Climate Data

For hydroclimate variables (precipitation, potential evapotranspiration, temperature), we used the ERA5-Land data, the fifth generation ECMWF (European Centre for Medium-Range Weather Forecasts) atmospheric reanalysis of the global climate, with a spatial resolution of 0.1°×0.1° and monthly temporal resolution (Smith, Tetzlaff, Kleine, Maneta, & Soulsby, 2021; Tarek, Brissette, & Arsenault, 2020). By using a higher spatial resolution (0.1° × 0.1°) than that of its driven climate reanalysis data (ERA5; 0.25° × 0.25°), ERA5-Land reanalysis datasets provide an improved representations of land surface processes (Muñoz, 2019).

To calculate the NAO and NCP indices, sea-level pressure (SLP) and 500 hPa geopotential height are derived from ERA5 datasets, with a spatial resolution of 0.25°×0.25°. Here, the NAO index is calculated using the 1st principal component (PC) of SLP anomalies over the North Atlantic (90°W-20°E, 20°-80°N) (Hurrell, 1995; Hurrell & Deser, 2009). The NCP index is the difference in the 500 hPa level geopotential height between the North Sea (0°, 55°N; 10°E, 55°N) and northern Caspian Sea (50°E, 45°N; 60°E, 45°N) region (Kutiel et al., 2002; Sezen, 2017). Here, ERA5-Land and ERA5 data have been extracted between 1981 and 2015 for consistency with the NDVI datasets.

We provide a comparison of precipitation patterns between the ERA5 and observation data from the Climate Research Unit (CRU: https://crudata.uea.ac.uk/cru/data/hrg/) in the Supplementary material (Figure S2). Generally, the annual summer and winter precipitation trends derived from ERA5 are consistent with that from CRU, with drying trends over eastern part of western Eurasia and wetting trends over western part (Figure S2). However, the CRU precipitation variability could be lower over the eastern part of western Eurasia, as the CRU dataset has fewer station data than ERA5 in some regions (Harris, Osborn, Jones, & Lister, 2020). Since we focus on the mechanism explaining co-variations in the NCP and dry/wet conditions in western Eurasia, such potential shortcomings should be neglectable.

2.3 Drought and vegetation indices

To quantify droughts and vegetation conditions, the SPI (McKee et al., 1993) and the NDVI are used. The SPI is calculated by assuming that precipitation is Gamma-distributed(Chun, 2010). As the growing season generally ranges from April to September (total 6 months) over western Eurasia, we use a 6-month aggregated SPI (i.e., SPI-6) (van Hateren et al., 2021). Nevertheless, the 1- to 12-month SPI time series have very similar patterns with the 6-month SPI results (not shown). To identify drought conditions, the SPI-6 < -1 is selected (van Hateren et al., 2021). To allow for a fair comparison between SPI-6 and NDVI, the NDVI is also standardized (hereafter called NDVI anomalies). The NDVI value less than -1 is also characterized as a significant vegetation decline.

2.4 Trend and the Generalised Least Square (GLS) regression

The Mann-Kendall (MK) test is used to quantify the significance of linear temporal trends nonparametrically (Kendall, 1975; Mann, 1945). Previous work argued that the results of the MK trend test could be misleading if serial correlations and outliers are ignored (Guo, Li, He, Xu, & Jin, 2018; Hamed, 2008; Hamed & Ramachandra Rao, 1998; Klaus, Chun, & Stumpp,

2015; Sang, Wang, & Liu, 2014). Thus, we use the modified MK test (Hamed & Ramachandra Rao, 1998) to examine trends of NDVI and hydroclimate variability. Trend intensity is estimated based on Thiel-Sen's slope, which is robust to outliers (Sen, 1968).

To explore the relationships between teleconnections, and water and vegetation distributions, GLS regressions are used, as in previous hydroclimate analysis (He et al., 2021; Klaus et al., 2015). The analytic GLS regressions can be written as

$$Y = \beta_0 + \beta_1 X \quad (1)$$

where Y is the climate variables or vegetation index, and X is the NCP index value. β_0 and β_1 are regression coefficients.

To consider spatial auto-correlation and the problem of multiplicity of spatial trend and regression results, we used a global significance test based on false discovery rate (FDR) as recommended in previous studies (Wilks, 2006, 2016). After estimating the *p*-values of trend and GLS regressions, the FDR test at p=0.05 is used to control the expected proportion of locally significant tests that are actually true, i.e. not occurring by chance due to spatial auto-correlation and the problem of multiplicity. A local significance test is rejected if the local *p*-value is no greater than:

$$P_{FDR} = \max_{j=1\to k} \left\{ p_{local}(j) : p_{local}(j) \leq \alpha_{FDR} \left(\frac{j}{k}\right) \right\} \quad (2)$$

where p_{local} (j) denotes the jth smallest (out of k) local p values, and the α_{FDR} is the chosen control level for the FDR (0.05 for this study).

2.5 Budyko framework

The Budyko framework has been used to examine long-term interactions among climate, regional hydrology and vegetation cover (Abera et al., 2019; Li et al., 2013; D. Zhang et al., 2018). There are different types of Budyko framework (Budyko (1974); Fu (1981); Choudhury (1999); H. Yang, Yang, Lei, and Sun (2008), which are summarised as follows:

Budyko (1974) $$\frac{\mathrm{ET}}{P} = \left[\frac{\mathrm{PET}}{P}\tanh\left(\frac{\mathrm{PET}}{P}\right)^{-1}\left(1-\exp\left(-\frac{\mathrm{PET}}{P}\right)\right)\right]^{0.5} \quad (2)$$

Fu (1981) $$\frac{ET}{P} = 1 + \frac{PET}{P} - \left[1 + \left(\frac{PET}{P}\right)^{\omega}\right]^{1/\omega} \quad (3)$$

Choudhury (1999); H. Yang et al. (2008) $$\frac{ET}{P} = \frac{1}{[1+(P+PET)^{\omega}]^{1/\omega}} \quad (4)$$

where ET, P and PET are land surface evapotranspiration, precipitation (water supply) and potential evapotranspiration (water demand), respectively, and ω is an empirical coefficient related to land patterns and characteristics.

Among these three equations (Equation 2-4), the one proposed by Fu (1981) is the most widely used. The Budyko space defines whether catchment state variations, processes and dynamics are water- or energy- limited based on precipitation (P), evapotranspiration (ET) and potential evapotranspiration (PET) (Berghuijs, Gnann, & Woods, 2020; Gentine, D'Odorico, Lintner, Sivandran, & Salvucci, 2012; Sposito, 2017). In the Budyko space, a Dryness Index (DI) (i.e., PET/P) value lower than 1 indicates a humid, energy-limited

environment, whereas a DI value higher than 1 indicates a dry, water-limited environment (Figure 2). The empirical coefficient ω is used to define and describe the relevant landscape characteristics, like climate and vegetation covers (Abera et al., 2019; C. Wang, Wang, Fu, & Zhang, 2016).

3 Results

3.1 Impact of NAO and NCP on meteorological drought and vegetation

We examine the relationships between two teleconnection patterns (i.e., NAO and NCP) and regional drought conditions over western Eurasia (Figure 3). There are no significant relationships between the DI, EI and the NAO, whereas the NCP is positively related to the DI and EI over western Eurasia (Figure 3). This indicates that positive NCP phases may better contribute to drier conditions over the region than the NAO. Moreover, based on the Budyko space (Figure S3b), the positive phases of NCP contribute to increasing dryness, thus causing the region to become more water-limited.

The NCP has significant negative impacts on precipitation over most western Eurasia, but positive impacts over central Asia (Figure S4). Regarding the temperature, NCP shows a negative relationship over the whole Eurasia (Figure S4). Such negative relationship with NCP is found over most parts of western Eurasia for PET, ET and NDVI variations. Generally, the NCP has negative impacts on meteorological and vegetation conditions over the region.

To further investigate how NCP affects regional drying/wetting conditions related to moisture circulations, we examine the regressed vertically integrated moisture flux associated with NCP variations (Figure 4). Positive NCP phases appear to promote anti-cyclonic circulation over the North Sea (closely adjacent to the continental western Eurasia), but cyclonic circulation anomalies over the Caspian Sea (Figure 4). Such circulation patterns are associated with drier condition over most part of the study region, but wetter condition over Central Asia.

3.2 Trends in meteorological and vegetation conditions

The mean SPI-6 values are positive and near to zero, suggesting that there is generally slightly humid air over most western Eurasia between 1981 and 2015 (Figure 5a). The mean state of NDVI shows dense vegetation cover (NDVI > 0.3) over most parts of western Eurasia, and sparse vegetation canopy (NDVI < 0.3) over Central Asia (Figure 5c). Between 1981 and 2015, there are generally significant decreasing trends in SPI-6 over western Eurasia except for the Italian Peninsula, Scandinavia and the Balkans (increasing trends; Figure 5b).

Regarding trends in vegetation cover, regions with dense vegetation cover (NDVI > 0.3) show increasing trends, and regions with sparse vegetation cover (NDVI < 0.3) show decreasing trends (Figure 5d). Therefore, green regions are becoming greener, and regions where vegetation coverage was low are becoming even less green. Interestingly, trend patterns in vegetation cover are not strictly following precipitation trend pattern. For instance, in western Russia and France, we can observe drier conditions concurrent with greening trends (Figure 5b, d).

3.3 Concomitance of meteorological drought and vegetation decline

To further explore the relationships between water deficits and vegetation growth, we examine the concurrence of meteorological drought and vegetation decline in Figure 6. Based on the SPI-6, we can identify five drought events that are particularly widespread (the area percentage is more than 50%; Figure S5): 1988, 1996, 2003, 2006, and 2010. Among these widespread drought events, the 1996 drought event appears as the most severe one, and therefore it is selected to analyse whether the meteorological drought and vegetation decline are concurrent (Figure 6; see Figures S6-S9 for other events). In April, both the SPI-6 and NDVI anomalies indicate a deficit in the Scandinavia, Baltic regions and western Russia, while this is only detected in the northernmost regions of Scandinavia in May (Figure 6a-b). Similar results are found in northern France and England, but in August and September (Figure 6e-f). In June and July, meteorological drought and vegetation decline do not occur simultaneously in most western Europe (Figure 6c-d). Generally, vegetation decline prevails in April and May, but hardly appears from June to September.

Based on the above results (Figure 6), western Russia and France are tend to become drier, but greener (Figure 5b, d). Here, we found that these regions are generally energy-limited (Figure 7), indicating that vegetation growth is mainly restricted by energy supply, and not by water supply (Gokmen, Vekerdy, Verhoef, & Batelaan, 2013; Parsons & Abrahams, 1994). Therefore, even though the region is drier, warmer temperatures promote vegetation growth. Scandinavia and Baltic regions are mainly water-limited (Figure 7), and thus the vegetation is very responsive to water deficits, and the NDVI declines as soon as water deficits occur (Figure 6a). In addition, considering for the whole of western Eurasia, all dots representing EI and DI values are approaching the energy-limited line (i.e. the line of EI=DI) in the Budyko space (Figure S5), suggesting that the whole region can be regarded as an energy-limited environment. Moreover, higher NDVI values correspond to higher EI and DI (Figure S5a), further confirming that drying condition may promote vegetation greenness in the energy-limited environment

4. Discussion

4.1 The role of teleconnection patterns on vegetation during droughts

NAO has been broadly accepted as the major mode causing hydrological and climate variability over western Eurasia (Lledó et al., 2020; Tsonis, Swanson, & Wang, 2008; W. Zhang et al., 2019). However, here, we demonstrated that NCP is a much better indicator for regional environmental changes over this region. The positive phases of NCP are related to an anticyclonic anomaly centred over the North Sea and a cyclonic anomaly is centred over the Caspian Sea region. NCP is indeed associated with moisture flux divergence, causing dryness over most parts of western Eurasia. Moreover, the positive phases of NCP are found to promote the drier continental airflow from northern Asia to affect the study region (Kutiel & Benaroch, 2002), contributing to the increased dryness. Such a negative relationship between NCP and winter precipitation has been previously reported over Turkey (Sezen, 2017). Sezen (2017), however, suggested that NCP is positively correlated with summer precipitation in some parts of Turkey. The difference of NCP impacts on precipitation could be related to the seasonal impacts. The negative relationships between NCP and precipitation in winter may be

too strong to mask the positive relationship in summer. Therefore, we found that the NCP has negative impacts on total precipitation of the whole year in this study. The seasonal impacts of NCP on regional climate variability require further investigation in future research work. In addition, the NCP has significant impacts on temperature (Brunetti & Kutiel, 2011), which may also contribute to vegetation growth. In addition, future studies should also examine the potential contribution of other large-scale climate modes of variability.

4.2 Similarity and disparity between drought conditions and vegetation patterns

Previous studies examined the relationship between droughts and vegetation growth in water- and energy-limited environments over Europe (Denissen et al., 2020; Peled et al., 2010; van Hateren et al., 2021). Peled et al. (2010) and van Hateren et al. (2021) found strong correlations between NDVI and drought indices in water-limited environments. We achieved similar results in our study: the meteorological droughts and vegetation decline occurred simultaneously over Scandinavia and Baltic regions, water-limited environments based on Budyko framework (Figure 5). However, the disparity in long-term variations in water quantity and vegetation density was not fully explained in previous studies. France and western Russia are getting drier during past decades. Therefore, one might expect vegetation to decline in response to such water deficits and thus NDVI values to decrease. However, this is not what we observed: NDVI values increased. France and western Russia are energy-limited according to the Budyko framework (Figure 5), which explains why vegetation is greening instead of suffering from the lack of water. In an energy-limited region, warmer temperatures promote vegetation growth, which is hypothesised to be due to enhancing photosynthesis activity (Dusenge, Duarte, & Way, 2019; L. Xu et al., 2013; D. Yang et al., 2021). However, if the precipitation deficits persist, we expect that vegetation growth will eventually be negatively affected. For instance, in 1996, the NDVI decreased in August and September over France after four months (April-July) of continuous precipitation deficits. The reason for the delayed vegetation responses might be due to large aquifer systems for water storage in this region (de Lavenne, Andréassian, Crochemore, Lindström, & Arheimer, 2021). Therefore, over France, the vegetation takes around four months before starting to decline after a precipitation deficit. Moreover, there are mostly croplands over France, and the irrigation for agriculture may also be the reason for the delayed vegetation responses (Foudi & Erdlenbruch, 2012; Sidibé, Terreaux, Tidball, & Reynaud, 2012).

4.3 Future implication for vegetation

Between 1981 and 2015, most parts of western Eurasia are energy-limited, and the vegetation growth is promoted by warmer temperatures via photosynthesis activity. However, as the climate is getting warmer, during the positive phase of NCP, we suggest here that the Eurasian ecosystem could reach a tipping point when warmer temperatures lead to a reduction in photosynthesis in the future (Moore et al., 2021; Slattery & Ort, 2019). In this case, many regions in Eurasia will have a transition to water-limited ecosystems and be more sensitive to drought risk (Bhuiyan, Saha, Bandyopadhyay, & Kogan, 2017; Tello-Garca et al., 2020). Therefore, the greening trend of vegetation will be unlikely to be continued sustainably in the future. Similarly, Rajczak and Schär (2017) projected the decrease in precipitation in the future over central Europe and France, and the increased droughts

negatively affect the forestry (Maracchi, Sirotenko, & Bindi, 2005). However, based on the IPCC report (IPCC, 2021), both precipitation and temperature are increasing under the global warming in the future, and such precipitation and temperature patterns can promote vegetation growth. Moreover, the climate impacts on vegetation can be quite different among regions related to the water-limited and energy-limited characteristics. Therefore, the future dynamic changes of vegetation in different regions need to be further studied.

5 Conclusions

In this study, we aim at exploring the similarity and disparity between meteorological drought conditions and vegetation pattern, and the role of teleconnection patterns on vegetation during droughts across western Eurasia. Trends in the SPI-6 and NDVI between 1981 and 2015 indicate contrasting results across different regions of western Eurasia. Specifically, while in northern and southeast regions, recent trends to wetter (drier) conditions are associated with an increase (decrease) in vegetation cover, other regions are paradoxically becoming greener while becoming drier. Such paradoxical patterns are found in energy-limited environmental systems based on the Budyko framework, where vegetation growth is primarily promoted by warmer temperature, enhancing photosynthesis activity. Moreover, the droughts and vegetation variability are suggested to be closely related to large-scale teleconnections. While previous studies have focused mostly on the impact of NAO, NCP, a relatively less studied teleconnections pattern, seems to explain better the variance of meteorological drought and vegetation response over western Eurasia.

The positive phases of NCP are demonstrated to contribute to the regional drying but greening trends over western Eurasia. Under the intensifying warming condition, due to the extra warmth brought by the positive phases of NCP, it will eventually lead the European ecosystem from energy-limited to be water-limited. As a result, the current trend of vegetation greening is unlikely to be sustained in the future. . Overall, we demonstrate an approach for investigating and forecasting droughts-vegetation changes based on emerging ecohydrological risk related to NCP which can be useful for regional land use and environment management.

Acknowledgement

This research was conducted using the resources of the High Performance Cluster Computing Centre, Hong Kong Baptist University, which receives funding from Research Grant Council, University Grant Committee of the HKSAR and Hong Kong Baptist University. The drought approach in the paper was developed from the PROCORE-France/Hong Kong Joint Research Scheme 2020/21 (F-HKBU201/20).

Data Availability Statement

The NDVI data that support the findings of this study are available in the the **National Aeronautics and Space Administration (NASA) ARC ECOCAST** (https://iridl.ldeo.columbia.edu/SOURCES/.NASA/.ARC/.ECOCAST/.GIMMS/.NDVI3g/.v1p0/index.html), and **NASA Land Processes Distributed Active Archive Center** (LP DAAC; https://e4ftl01.cr.usgs.gov/MOLT/MOD13C2.006/). The climate data that support

the findings of this study are openly available in **ERA5-Land monthly averaged data from 1981 to present** at http://doi.org/10.24381/cds.68d2bb30, **ERA5 monthly averaged data on single levels from 1979 to present** at http://doi.org/10.24381/cds.f17050d7, the **Climate Research Unit** (CRU; https://crudata.uea.ac.uk/cru/data/hrg/).

References

Abera, W., Tamene, L., Abegaz, A., & Solomon, D. (2019). Understanding climate and land surface changes impact on water resources using Budyko framework and remote sensing data in Ethiopia. *Journal of Arid Environments, 167*, 56-64. doi:https://doi.org/10.1016/j.jaridenv.2019.04.017

Alpert, P., Baldi, M., Ilani, R., Krichak, S., Price, C., Rodó, X., . . . Xoplaki, E. (2006). Chapter 2 Relations between climate variability in the Mediterranean region and the tropics: ENSO, South Asian and African monsoons, hurricanes and Saharan dust. In P. Lionello, P. Malanotte-Rizzoli, & R. Boscolo (Eds.), *Developments in Earth and Environmental Sciences* (Vol. 4, pp. 149-177): Elsevier.

Bachmair, S., Tanguy, M., Hannaford, J., & Stahl, K. (2018). How well do meteorological indicators represent agricultural and forest drought across Europe? *Environmental Research Letters, 13*(3). doi:10.1088/1748-9326/aaafda

Báez, J. C., Real, R., López-Rodas, V., Costas, E., Salvo, A. E., García-Soto, C., & Flores-Moya, A. (2014). The North Atlantic Oscillation and the Arctic Oscillation favour harmful algal blooms in SW Europe. *Harmful Algae, 39*, 121-126. doi:https://doi.org/10.1016/j.hal.2014.07.008

Berghuijs, W. R., Gnann, S. J., & Woods, R. A. (2020). Unanswered questions on the Budyko framework. *Hydrological Processes, 34*(26), 5699--5703. doi:10.1002/hyp.13958

Bhuiyan, C., Saha, A. K., Bandyopadhyay, N., & Kogan, F. N. (2017). Analyzing the impact of thermal stress on vegetation health and agricultural drought–a case study from Gujarat, India. *GIScience and Remote Sensing, 54*(5), 678--699. doi:10.1080/15481603.2017.1309737

Brunetti, M., & Kutiel, H. (2011). The relevance of the North-Sea Caspian Pattern (NCP) in explaining temperature variability in Europe and the Mediterranean. *Nat. Hazards Earth Syst. Sci., 11*(10), 2881-2888. doi:10.5194/nhess-11-2881-2011

Budyko, M. I. (1974). *Climate and life*: Academic Press New York.

Buitink, J., & Swank, A. M. a. (2020). Anatomy of the 2018 agricultural drought in the Netherlands using in situ soil moisture and satellite vegetation indices. *Hydrology and Earth System Sciences, 24*(12), 6021--6031. doi:10.5194/hess-24-6021-2020

Buras, A., & Rammig, A. a. (2020). Quantifying impacts of the 2018 drought on European ecosystems in comparison to 2003. *Biogeosciences, 17*(6), 1655--1672. doi:10.5194/bg-17-1655-2020

Çağlar, F., Yetemen, O., Pan Chun, K., & Lutfi Sen, O. (2021, 2021/04/1). *Applicability of the North Sea Caspian Pattern as an indicator of the Euro-Mediterranean Climate Variability*.

Cai, D., Fraedrich, K., Sielmann, F., Guan, Y., Guo, S., Zhang, L., & Zhu, X. (2014). Climate and vegetation: An ERA-Interim and GIMMS NDVI analysis. *Journal of Climate, 27*(13), 5111--5118. doi:10.1175/JCLI-D-13-00674.1

Cancelliere, A., Mauro, G. D., Bonaccorso, B., & Rossi, G. (2007). Drought forecasting using the standardized precipitation index. *Water Resources Management, 21*(5), 801--819. doi:10.1007/s11269-006-9062-y

Changnon, S. A. (2003). Present and future economic impacts of climate extremes in the united states. *Environmental Hazards, 5*(2), 47--50. doi:10.1016/j.hazards.2004.04.001

Choudhury, B. J. (1999). Evaluation of an empirical equation for annual evaporation using field observations and results from a biophysical model. *Journal of Hydrology, 216*(1-2), 99--110. doi:10.1016/S0022-1694(98)00293-5

Chun, K. P. (2010). *Statistical downscaling of climate model outputs for hydrological extremes.* (Doctoral), Imperial College London. Retrieved from http://hdl.handle.net/10044/1/6972

Creed, I. F., Spargo, A. T., Jones, J. A., Buttle, J. M., Adams, M. B., Beall, F. D., . . . Yao, H. (2014). Changing forest water yields in response to climate warming: results from long-term experimental watershed sites across North America. *Global Change Biology, 20*(10), 3191-3208. doi:https://doi.org/10.1111/gcb.12615

de Lavenne, A., Andréassian, V., Crochemore, L., Lindström, G., & Arheimer, B. (2021). Quantifying pluriannual hydrological memory with Catchment Forgetting Curves. *Hydrol. Earth Syst. Sci. Discuss., 2021*, 1-27. doi:10.5194/hess-2021-331

Denissen, J. M. C., Teuling, A. J., Reichstein, M., & Orth, R. (2020). Critical Soil Moisture Derived From Satellite Observations Over Europe. *Journal of Geophysical Research: Atmospheres, 125*(6), e2019JD031672. doi:https://doi.org/10.1029/2019JD031672

Deser, C., Hurrell, J. W., & Phillips, A. S. (2017). The role of the North Atlantic Oscillation in European climate projections. *Climate Dynamics, 49*(9), 3141-3157. doi:10.1007/s00382-016-3502-z

Dippner, J. W., Möller, C., & Hänninen, J. (2012). Regime shifts in North Sea and Baltic Sea: A comparison. *Journal of Marine Systems, 105-108*, 115-122. doi:https://doi.org/10.1016/j.jmarsys.2012.07.001

Dusenge, M. E., Duarte, A. G., & Way, D. A. (2019). Plant carbon metabolism and climate change: elevated CO2 and temperature impacts on photosynthesis, photorespiration and respiration. *New Phytologist, 221*(1), 32-49. doi:https://doi.org/10.1111/nph.15283

Fensholt, R., & Proud, S. R. (2012). Evaluation of Earth Observation based global long term vegetation trends — Comparing GIMMS and MODIS global NDVI time series. *Remote Sensing of Environment, 119*, 131-147. doi:https://doi.org/10.1016/j.rse.2011.12.015

Foudi, S., & Erdlenbruch, K. (2012). The role of irrigation in farmers' risk management strategies in France. *European Review of Agricultural Economics, 39*(3), 439-457. doi:10.1093/erae/jbr024

Fu, B. (1981). On the calculation of the evaporation from land surface. *Sci. Atmos. Sin, 5*(1), 23-31.

Gentine, P., D'Odorico, P., Lintner, B. R., Sivandran, G., & Salvucci, G. (2012). Interdependence of climate, soil, and vegetation as constrained by the Budyko curve. *Geophysical Research Letters, 39*(19). doi:10.1029/2012GL053492

Gokmen, M., Vekerdy, Z., Verhoef, W., & Batelaan, O. (2013). Satellite-based analysis of recent trends in the ecohydrology of a semi-arid region. *Hydrol. Earth Syst. Sci., 17*(10), 3779-3794. doi:10.5194/hess-17-3779-2013

Gouveia, C., Trigo, R. M., DaCamara, C. C., Libonati, R., & Pereira, J. M. C. (2008). The North Atlantic Oscillation and European vegetation dynamics. *International Journal of Climatology, 28*(14), 1835-1847. doi:https://doi.org/10.1002/joc.1682

Guo, M., Li, J., He, H., Xu, J., & Jin, Y. (2018). Detecting Global Vegetation Changes Using Mann-Kendal (MK) Trend Test for 1982–2015 Time Period. *Chinese Geographical Science, 28*(6), 907-919. doi:10.1007/s11769-018-1002-2

Hamed, K. H. (2008). Trend detection in hydrologic data: The Mann–Kendall trend test under the scaling hypothesis. *Journal of Hydrology, 349*(3), 350-363. doi:https://doi.org/10.1016/j.jhydrol.2007.11.009

Hamed, K. H., & Ramachandra Rao, A. (1998). A modified Mann-Kendall trend test for autocorrelated data. *Journal of Hydrology, 204*(1), 182-196. doi:https://doi.org/10.1016/S0022-1694(97)00125-X

Harris, I., Osborn, T. J., Jones, P., & Lister, D. (2020). Version 4 of the CRU TS monthly high-resolution gridded multivariate climate dataset. *Scientific data, 7*(1), 109-109. doi:10.1038/s41597-020-0453-3

He, Q., Chun, K. P., Tan, M. L., Dieppois, B., Liew, J., Klaus, J., . . . Yetemen, O. (2021). Tropical drought patterns and their linkages to large-scale climate variability over Peninsular Malaysia. *Hydrological Processes, n/a*(n/a), e14356. doi:https://doi.org/10.1002/hyp.14356

Hu, X., Ren, H., Tansey, K., Zheng, Y., Ghent, D., Liu, X., & Yan, L. (2019). Agricultural drought monitoring using European Space Agency Sentinel 3A land surface temperature and normalized difference vegetation index imageries. *Agricultural and Forest Meteorology, 279*, 107707. doi:10.1016/j.agrformet.2019.107707

Hurrell, J. W. (1995). Decadal Trends in the North Atlantic Oscillation: Regional Temperatures and Precipitation. *Science, 269*(5224), 676. doi:10.1126/science.269.5224.676

Hurrell, J. W., & Deser, C. (2009). North Atlantic climate variability: The role of the North Atlantic Oscillation. *Journal of Marine Systems, 78*(1), 28-41. doi:https://doi.org/10.1016/j.jmarsys.2008.11.026

Iles, C., & Hegerl, G. (2017). Role of the North Atlantic Oscillation in decadal temperature trends. *Environmental Research Letters, 12*(11), 114010. doi:10.1088/1748-9326/aa9152

Ionita, M. (2014). The Impact of the East Atlantic/Western Russia Pattern on the Hydroclimatology of Europe from Mid-Winter to Late Spring. *Climate, 2*(4). doi:10.3390/cli2040296

Ionita, M., Tallaksen, L., Kingston, D., Stagge, J., Laaha, G., Van Lanen, H., . . . Haslinger, K. (2017). The European 2015 drought from a climatological perspective. *Hydrology and Earth System Sciences, 21*, 1397-1419. doi:doi:10.5194/hess-21-1397-2017

IPCC. (2021). *Summary for Policymakers*. Retrieved from

Kendall, M. G. (1975). *Rank correlation methods*. Oxford, England: Griffin.

Klaus, J., Chun, K. P., & Stumpp, C. (2015). Temporal trends in δ18O composition of

precipitation in Germany: insights from time series modelling and trend analysis. *Hydrological Processes, 29*(12), 2668-2680. doi:10.1002/hyp.10395

Kutiel, H., & Benaroch, Y. (2002). North Sea-Caspian Pattern (NCP) – an upper level atmospheric teleconnection affecting the Eastern Mediterranean: Identification and definition. *Theoretical and applied climatology, 71*(1), 17-28. doi:10.1007/s704-002-8205-x

Kutiel, H., Maheras, P., Türkeş, M., & Paz, S. (2002). North Sea – Caspian Pattern (NCP) – an upper level atmospheric teleconnection affecting the eastern Mediterranean – implications on the regional climate. *Theoretical and Applied Climatology, 72*(3), 173-192. doi:10.1007/s00704-002-0674-8

Kutiel, H., & Türkeş, M. (2005). New evidence for the role of the north sea — caspian pattern on the temperature and precipitation regimes in continental central turkey. *Geografiska Annaler: Series A, Physical Geography, 87*(4), 501-513. doi:10.1111/j.0435-3676.2005.00274.x

Lee, D. Y., Lin, W., & Petersen, M. R. (2020). Wintertime Arctic Oscillation and North Atlantic Oscillation and their impacts on the Northern Hemisphere climate in E3SM. *Climate Dynamics, 55*(5), 1105-1124. doi:10.1007/s00382-020-05316-0

Lee, R. W., Woolnough, S. J., Charlton-Perez, A. J., & Vitart, F. (2019). ENSO Modulation of MJO Teleconnections to the North Atlantic and Europe. *Geophysical Research Letters, 46*(22), 13535-13545. doi:https://doi.org/10.1029/2019GL084683

Li, D., Pan, M., Cong, Z., Zhang, L., & Wood, E. (2013). Vegetation control on water and energy balance within the Budyko framework. *Water Resources Research, 49*(2), 969-976. doi:https://doi.org/10.1002/wrcr.20107

Lian, X., Piao, S., Chen, A., Huntingford, C., Fu, B., Li, L. Z. X., . . . Roderick, M. L. (2021). Multifaceted characteristics of dryland aridity changes in a warming world. *Nature Reviews Earth & Environment, 2*(4), 232-250. doi:10.1038/s43017-021-00144-0

Livada, I., & Assimakopoulos, V. D. (2007). Spatial and temporal analysis of drought in Greece using the Standardized Precipitation Index (SPI). *Theoretical and applied climatology, 89*(3-4), 143--153. doi:10.1007/s00704-005-0227-z

Lledó, L., Cionni, I., Torralba, V., Bretonnière, P.-A., & Samsó, M. (2020). Seasonal prediction of Euro-Atlantic teleconnections from multiple systems. *Environmental Research Letters, 15*(7), 074009. doi:10.1088/1748-9326/ab87d2

Mann, H. B. (1945). Nonparametric Tests Against Trend. *Econometrica, 13*(3), 245-259. doi:10.2307/1907187

Maracchi, G., Sirotenko, O., & Bindi, M. (2005). Impacts of Present and Future Climate Variability on Agriculture and Forestry in the Temperate Regions: Europe. *Climatic Change, 70*(1), 117-135. doi:10.1007/s10584-005-5939-7

McKee, T. B., Doesken, N. J., & Kleist, J. (1993). *The relationship of drought frequency and duration to time scales.* Paper presented at the Proceedings of the 8th Conference on Applied Climatology.

Measho, S., Chen, B., Trisurat, Y., Pellikka, P., Guo, L., Arunyawat, S., . . . Yemane, T. (2019). Spatio-Temporal Analysis of Vegetation Dynamics as a Response to Climate Variability and Drought Patterns in the Semiarid Region, Eritrea. *Remote Sensing, 11*(6), 724. doi:10.3390/rs11060724

Mezzina, B., García-Serrano, J., Bladé, I., & Kucharski, F. (2020). Dynamics of the ENSO Teleconnection and NAO Variability in the North Atlantic–European Late Winter. *Journal of Climate, 33*(3), 907-923. doi:10.1175/JCLI-D-19-0192.1

Mikolaskova, K. (2009). Continental and oceanic precipitation régime in Europe. *Central European Journal of Geosciences, 1*(2), 176-182. doi:10.2478/v10085-009-0013-8

Moore, C. E., Meacham-Hensold, K., Lemonnier, P., Slattery, R. A., Benjamin, C., Bernacchi, C. J., . . . Cavanagh, A. P. (2021). The effect of increasing temperature on crop photosynthesis: from enzymes to ecosystems. *Journal of Experimental Botany, 72*(8), 2822-2844. doi:10.1093/jxb/erab090

Muñoz, S., J. (2019). *C3S ERA5-Land reanalysis*. Retrieved from: https://cds.climate.copernicus.eu/cdsapp#!/home

Murnane, R. J. (2004). Climate research and reinsurance. *Bulletin of the American Meteorological Society, 85*(5), 697--707. doi:10.1175/BAMS-85-5-697

Niu, J., Kang, S., Zhang, X., & Fu, J. (2019). Vulnerability analysis based on drought and vegetation dynamics. *Ecological Indicators, 105*, 329--336. doi:10.1016/j.ecolind.2017.10.048

Olafsson, H., & Rousta, I. (2021). Influence of atmospheric patterns and North Atlantic Oscillation (NAO) on vegetation dynamics in Iceland using Remote Sensing. *European Journal of Remote Sensing, 54*(1), 351-363. doi:10.1080/22797254.2021.1931462

Parmesan, C., Root, T. L., & Willig, M. R. (2000). Impacts of extreme weather and climate on terrestrial biota. *Bulletin of the American Meteorological Society, 81*(3), 443--450. doi:10.1175/1520-0477(2000)081<0443:IOEWAC>2.3.CO;2

Parsons, A. J., & Abrahams, A. D. (1994). Geomorphology of Desert Environments. In A. D. Abrahams & A. J. Parsons (Eds.), *Geomorphology of Desert Environments* (pp. 3-12). Dordrecht: Springer Netherlands.

Peled, E., Dutra, E., Viterbo, P., & Angert, A. (2010). Technical Note: Comparing and ranking soil drought indices performance over Europe, through remote-sensing of vegetation. *Hydrol. Earth Syst. Sci., 14*(2), 271-277. doi:10.5194/hess-14-271-2010

Peng, S., Chen, A., Xu, L., Cao, C., Fang, J., Myneni, R. B., . . . Piao, S. (2011). Recent change of vegetation growth trend in China. *Environmental Research Letters, 6*(4), 044027. doi:10.1088/1748-9326/6/4/044027

Pinzon, J. E., & Tucker, C. J. (2014). A Non-Stationary 1981–2012 AVHRR NDVI3g Time Series. *Remote Sensing, 6*(8). doi:10.3390/rs6086929

Rajczak, J., & Schär, C. (2017). Projections of Future Precipitation Extremes Over Europe: A Multimodel Assessment of Climate Simulations. *Journal of Geophysical Research: Atmospheres, 122*(20), 10,773-710,800. doi:https://doi.org/10.1002/2017JD027176

Rimkus, E., Stonevicius, E., Kilpys, J., MacIulyte, V., & Valiukas, D. (2017). Drought identification in the eastern Baltic region using NDVI. *Earth System Dynamics, 8*(3), 627--637. doi:10.5194/esd-8-627-2017

Rousi, E., Rust, H. W., Ulbrich, U., & Anagnostopoulou, C. (2020). Implications of winter NAO flavors on present and future European climate. *Climate, 8*(1), 13. doi:10.3390/cli8010013

Rust, W., Holman, I., Corstanje, R., Bloomfield, J., & Cuthbert, M. (2018). A conceptual

model for climatic teleconnection signal control on groundwater variability in Europe (Vol. 177, pp. 164--174).

Sang, Y.-F., Wang, Z., & Liu, C. (2014). Comparison of the MK test and EMD method for trend identification in hydrological time series. *Journal of Hydrology, 510*, 293-298. doi:https://doi.org/10.1016/j.jhydrol.2013.12.039

Sawada, Y. (2018). Quantifying drought propagation from soil moisture to vegetation dynamics using a newly developed ecohydrological land reanalysis. *Remote Sensing, 10*(8). doi:10.3390/rs10081197

Sen, P. K. (1968). Estimates of the Regression Coefficient Based on Kendall's Tau. *Journal of the American Statistical Association, 63*(324), 1379-1389. doi:10.1080/01621459.1968.10480934

Sepulcre-Canto, G., Horion, S., Singleton, A., Carrao, H., & Vogt, J. (2012). Development of a Combined Drought Indicator to detect agricultural drought in Europe (Vol. 12, pp. 3519--3531).

Sezen, C. (2017). The Relation of North Atlantic Oscillation (NAO) and North Sea Caspian Pattern (NCP) With Climate Variables in Mediterranean Region of Turkey. *The Eurasia Proceedings of Science Technology Engineering and Mathematics, 1*, 366--371.

Sezen, C., & Partal, T. (2019). The impacts of Arctic oscillation and the North Sea Caspian pattern on the temperature and precipitation regime in Turkey. *Meteorology and Atmospheric Physics, 131*(6), 1677--1696. doi:10.1007/s00703-019-00665-w

Sibley, A., Cox, D., & Titley, H. (2015). Coastal flooding in England and Wales from Atlantic and North Sea storms during the 2013/2014 winter. *Weather, 70*(2), 62-70. doi:https://doi.org/10.1002/wea.2471

Sidibé, Y., Terreaux, J.-P., Tidball, M., & Reynaud, A. (2012). Coping with drought with innovative pricing systems: the case of two irrigation water management companies in France. *Agricultural Economics, 43*(s1), 141-155. doi:https://doi.org/10.1111/j.1574-0862.2012.00628.x

Slattery, R. A., & Ort, D. R. (2019). Carbon assimilation in crops at high temperatures. *Plant, Cell & Environment, 42*(10), 2750-2758. doi:https://doi.org/10.1111/pce.13572

Smith, A., Tetzlaff, D., Kleine, L., Maneta, M., & Soulsby, C. (2021). Quantifying the effects of land use and model scale on water partitioning and water ages using tracer-aided ecohydrological models. *Hydrology and Earth System Sciences, 25*(4), 2239--2259. doi:10.5194/hess-25-2239-2021

Solano, R., Didan, K., Jacobson, A., & Huete, A. (2010). MODIS Vegetation Index User ' s Guide (MOD13 Series). *The University of Arizona, 2010*(May), 38.

Sposito, G. (2017). Understanding the budyko equation. *Water (Switzerland), 9*(4), 1--14. doi:10.3390/w9040236

Stampoulis, D., & Anagnostou, E. (2012). Evaluation of global satellite rainfall products over Continental Europe. *Journal of Hydrometeorology, 13*(2), 588--603. doi:10.1175/JHM-D-11-086.1

Sutanto, S. J., van der Weert, M., Wanders, N., & Blauhut, V. a. (2019). Moving from drought hazard to impact forecasts. *Nature Communications, 10*(1), 1--7. doi:10.1038/s41467-019-12840-z

Tarek, M., Brissette, F. P., & Arsenault, R. (2020). Evaluation of the ERA5 reanalysis as a potential reference dataset for hydrological modelling over North America. *Hydrol. Earth Syst. Sci., 24*(5), 2527-2544. doi:10.5194/hess-24-2527-2020

Tello-Garca, E., Huber, L., Leitinger, G., Peters, A., Newesely, C., Ringler, M. E., & Tasser, E. (2020). Drought- and heat-induced shifts in vegetation composition impact biomass production and water use of alpine grasslands. *Environmental and Experimental Botany, 169*, 103921. doi:10.1016/j.envexpbot.2019.103921

Teuling, A. J. a. (2013). Evapotranspiration amplifies European summer drought. *Geophysical Research Letters, 40*(10), 2071--2075. doi:10.1002/grl.50495

Toreti, A., Desiato, F., Fioravanti, G., & Perconti, W. (2010). Seasonal temperatures over Italy and their relationship with low-frequency atmospheric circulation patterns. *Climatic Change, 99*(1), 211-227. doi:10.1007/s10584-009-9640-0

Tošić, I., & Putniković, S. (2021). Influence of the East Atlantic/West Russia pattern on precipitation over Serbia. *Theoretical and Applied Climatology, 146*(3), 997-1006. doi:10.1007/s00704-021-03777-9

Tsanis, I., & Tapoglou, E. (2019). Winter North Atlantic Oscillation impact on European precipitation and drought under climate change. *Theoretical and Applied Climatology, 135*(1), 323-330. doi:10.1007/s00704-018-2379-7

Tsonis, A. A., Swanson, K. L., & Wang, G. (2008). On the role of atmospheric teleconnections in climate. *Journal of Climate, 21*(12), 2990--3001. doi:10.1175/2007JCLI1907.1

Ulbrich, U., Lionello, P., Belušić, D., Jacobeit, J., Knippertz, P., Kuglitsch, F. G., . . . Ziv, B. (2012). 5 - Climate of the Mediterranean: Synoptic Patterns, Temperature, Precipitation, Winds, and Their Extremes. In P. Lionello (Ed.), *The Climate of the Mediterranean Region* (pp. 301-346). Oxford: Elsevier.

van Hateren, T. C., Chini, M., Matgen, P., & Teuling, A. J. (2021). Ambiguous Agricultural Drought: Characterising Soil Moisture and Vegetation Droughts in Europe from Earth Observation. *Remote Sensing, 13*(10). doi:10.3390/rs13101990

Wang, C., Wang, S., Fu, B., & Zhang, L. (2016). Advances in hydrological modelling with the Budyko framework: A review. *Progress in Physical Geography, 40*(3), 409--430. doi:10.1177/0309133315620997

Wang, X., Wang, T., Liu, D., Guo, H., Huang, H., & Zhao, Y. (2017). Moisture-induced greening of the South Asia over the past three decades. *Global Change Biology, 23*(11), 4995-5005. doi:10.1111/gcb.13762

Wilks, D. S. (2006). On "Field Significance" and the False Discovery Rate. *Journal of Applied Meteorology and Climatology, 45*(9), 1181-1189. doi:10.1175/JAM2404.1

Wilks, D. S. (2016). "The Stippling Shows Statistically Significant Grid Points": How Research Results are Routinely Overstated and Overinterpreted, and What to Do about It. *Bulletin of the American Meteorological Society, 97*(12), 2263-2273. doi:10.1175/BAMS-D-15-00267.1

Wu, D., Qu, J. J., & Hao, X. (2015). Agricultural drought monitoring using MODIS-based drought indices over the USA Corn Belt. *International journal of remote sensing, 36*(21), 5403--5425. doi:10.1080/01431161.2015.1093190

Wu, D., Wu, H., Zhao, X., Zhou, T., Tang, B., Zhao, W., & Jia, K. (2014). Evaluation of

spatiotemporal variations of global fractional vegetation cover based on GIMMS NDVI data from 1982 to 2011. *Remote Sensing, 6*(5), 4217--4239. doi:10.3390/rs6054217

Xu, G., Zhang, H., Chen, B., Zhang, H., Innes, J. L., Wang, G., . . . Myneni, R. B. (2014). Changes in Vegetation Growth Dynamics and Relations with Climate over China's Landmass from 1982 to 2011. *Remote Sensing, 6*(4). doi:10.3390/rs6043263

Xu, L., Myneni, R. B., Chapin Iii, F. S., Callaghan, T. V., Pinzon, J. E., Tucker, C. J., . . . Stroeve, J. C. (2013). Temperature and vegetation seasonality diminishment over northern lands. *Nature Climate Change, 3*(6), 581-586. doi:10.1038/nclimate1836

Yang, D., Xu, X., Xiao, F., Xu, C., Luo, W., & Tao, L. (2021). Improving modeling of ecosystem gross primary productivity through re-optimizing temperature restrictions on photosynthesis. *Science of The Total Environment, 788*, 147805. doi:https://doi.org/10.1016/j.scitotenv.2021.147805

Yang, H., Yang, D., Lei, Z., & Sun, F. (2008). New analytical derivation of the mean annual water-energy balance equation. *Water Resources Research, 44*(3), 3410. doi:10.1029/2007WR006135

Zhang, D., Liu, X., & Bai, P. (2018). Different influences of vegetation greening on regional water-energy balance under different climatic conditions. *Forests, 9*(7), 1--15. doi:10.3390/f9070412

Zhang, W., Wang, Z., Stuecker, M. F., Turner, A. G., Jin, F. F., & Geng, X. (2019). Impact of ENSO longitudinal position on teleconnections to the NAO. *Climate Dynamics, 52*(1-2), 257--274. doi:10.1007/s00382-018-4135-1

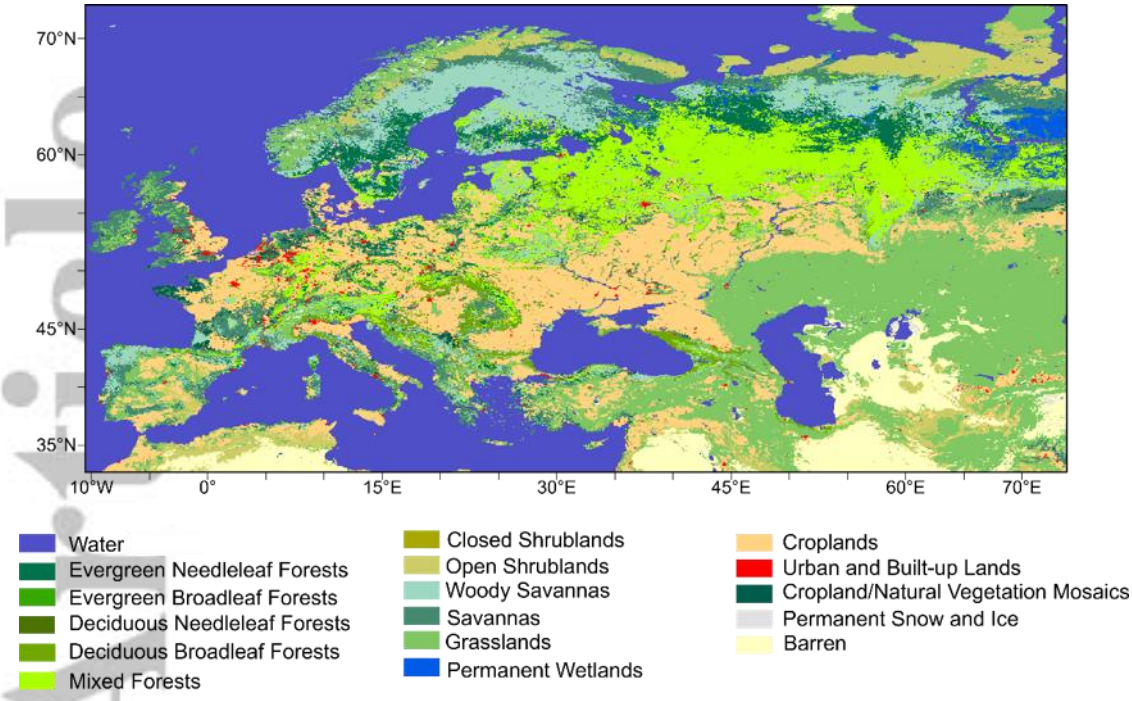

Figure 1. The land cover types over the western continental Eurasia between 10°W-70°E and 35°N-72°N.

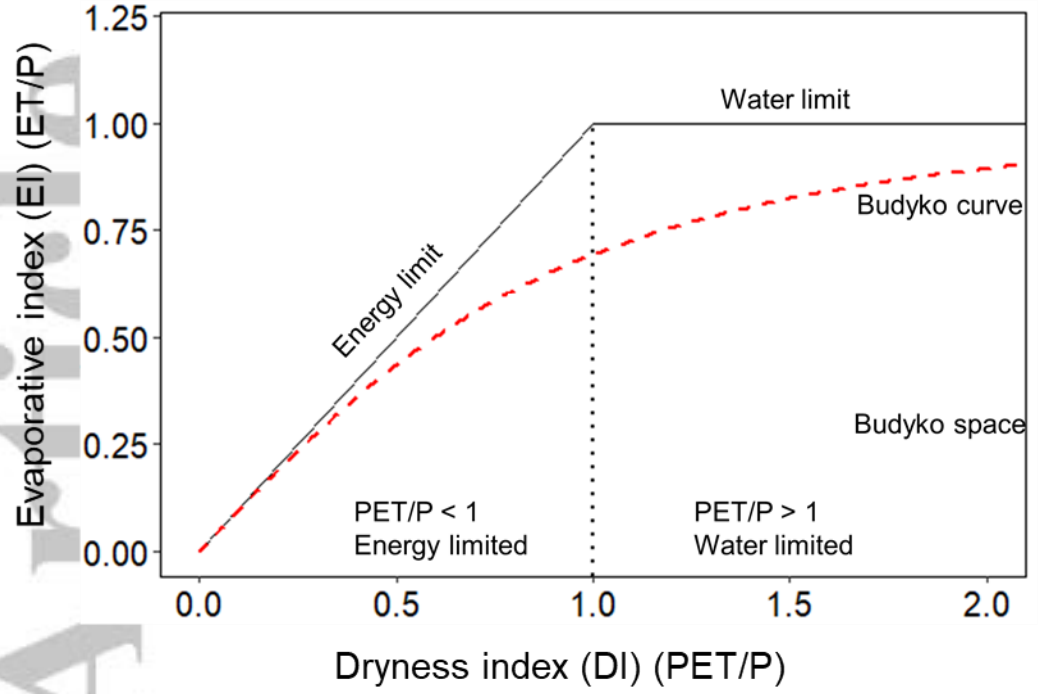

Figure 2. Budyko framework (dryness index against evaporative index). The solid lines indicate the energy limit and water limit boundaries. The red dashed line is the theoretical Budyko curve with a default ω value (i.e., 2.6; Creed et al., 2014).

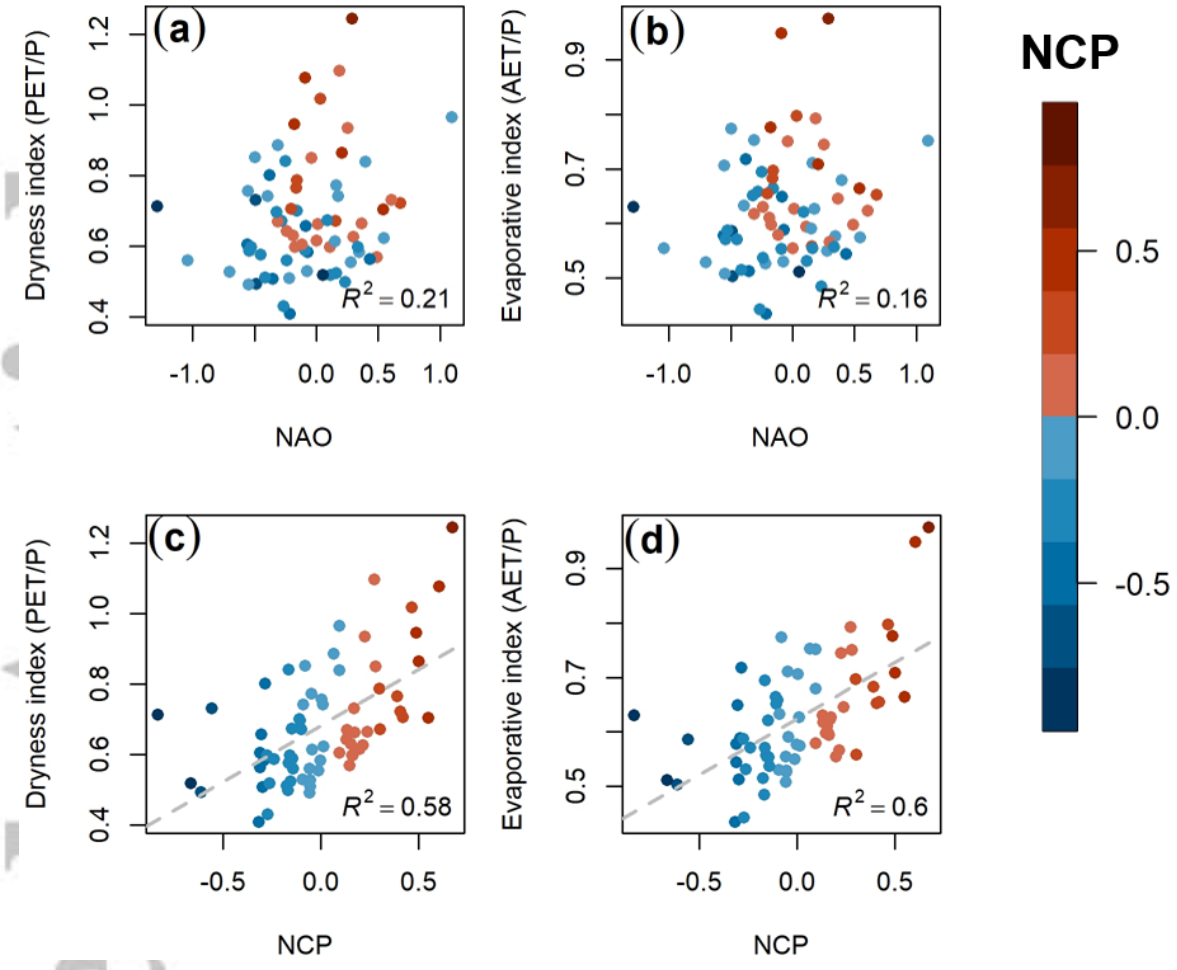

Figure 3. The NAO against DI (a) and EI (b) between 1981 and 2015. (c-d) are same as (a-b) but for NCP. Red and blue colours indicate the positive and negative phases of NAO/NCP, respectively. The colorbar indicates the NCP values.

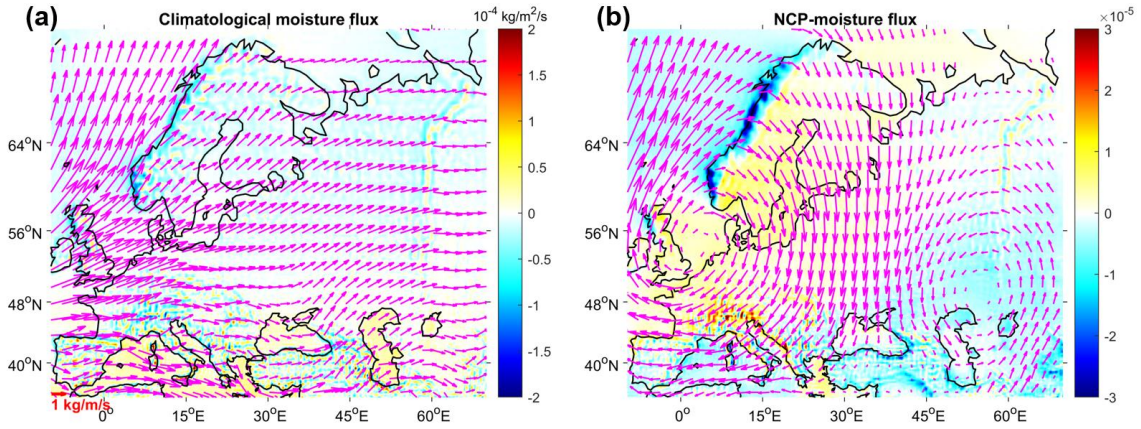

Figure 4. Vertically integrated moisture flux and divergence climatological state (a) and regressed map with NCP (b) between 1981 and 2015. For (a), the magenta arrows and shaded area are climatological moisture flux and moisture flux divergence, respectively. For (b), the arrows and shaded areas represent the regressed coefficients of moisture flux and regressed coefficients of moisture flux divergence, respectively. For regression map, only significant results at $p \leqslant 0.05$ according to the local significance test, and to the FDR global significance test are shown (Wilks, 2006, 2016).

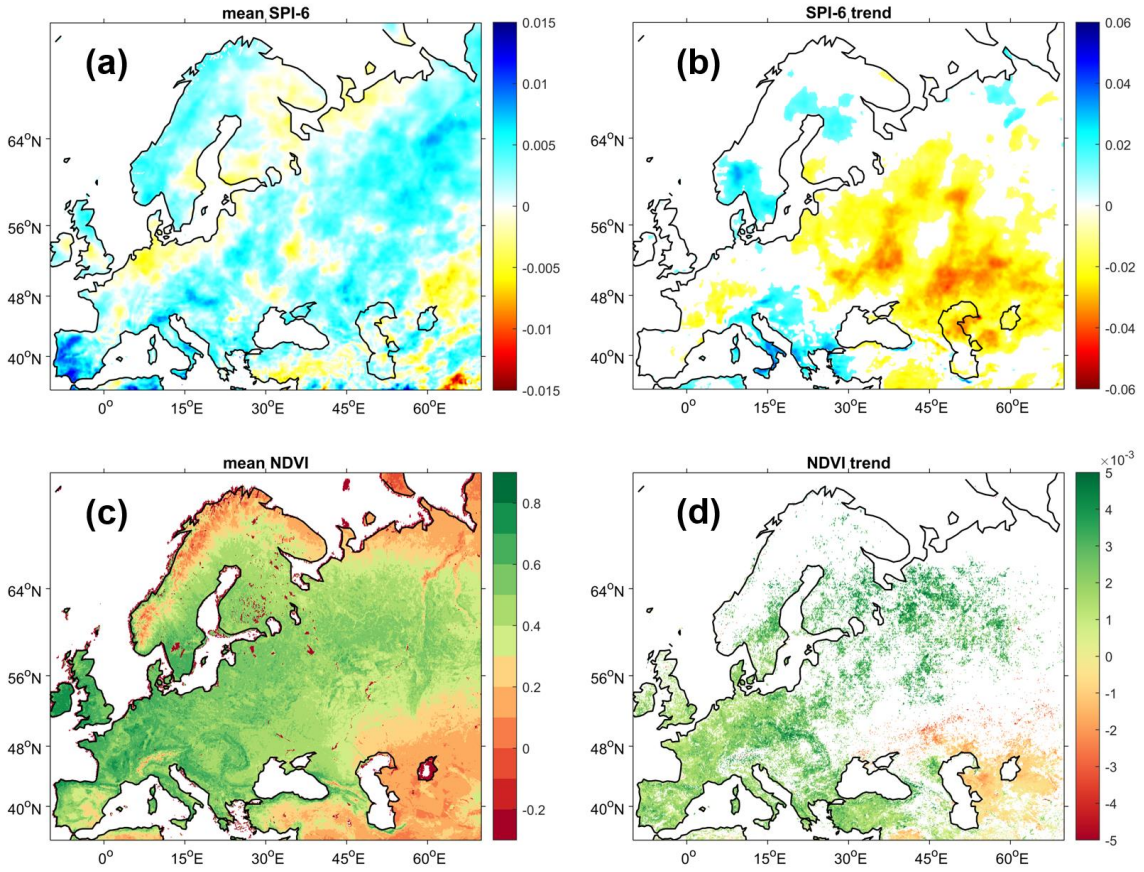

Figure 5. The mean state (a) and trend (b) of SPI-6 and NDVI (c-d) between 1981 and 2015 over western Eurasia. Trend maps only show results that are statistically significant at $p \leq 0.05$ according to the MK trend test, and to the FDR global significance test (Wilks, 2006, 2016). For trend maps, the colorbar refers to the slope value of trend analysis.

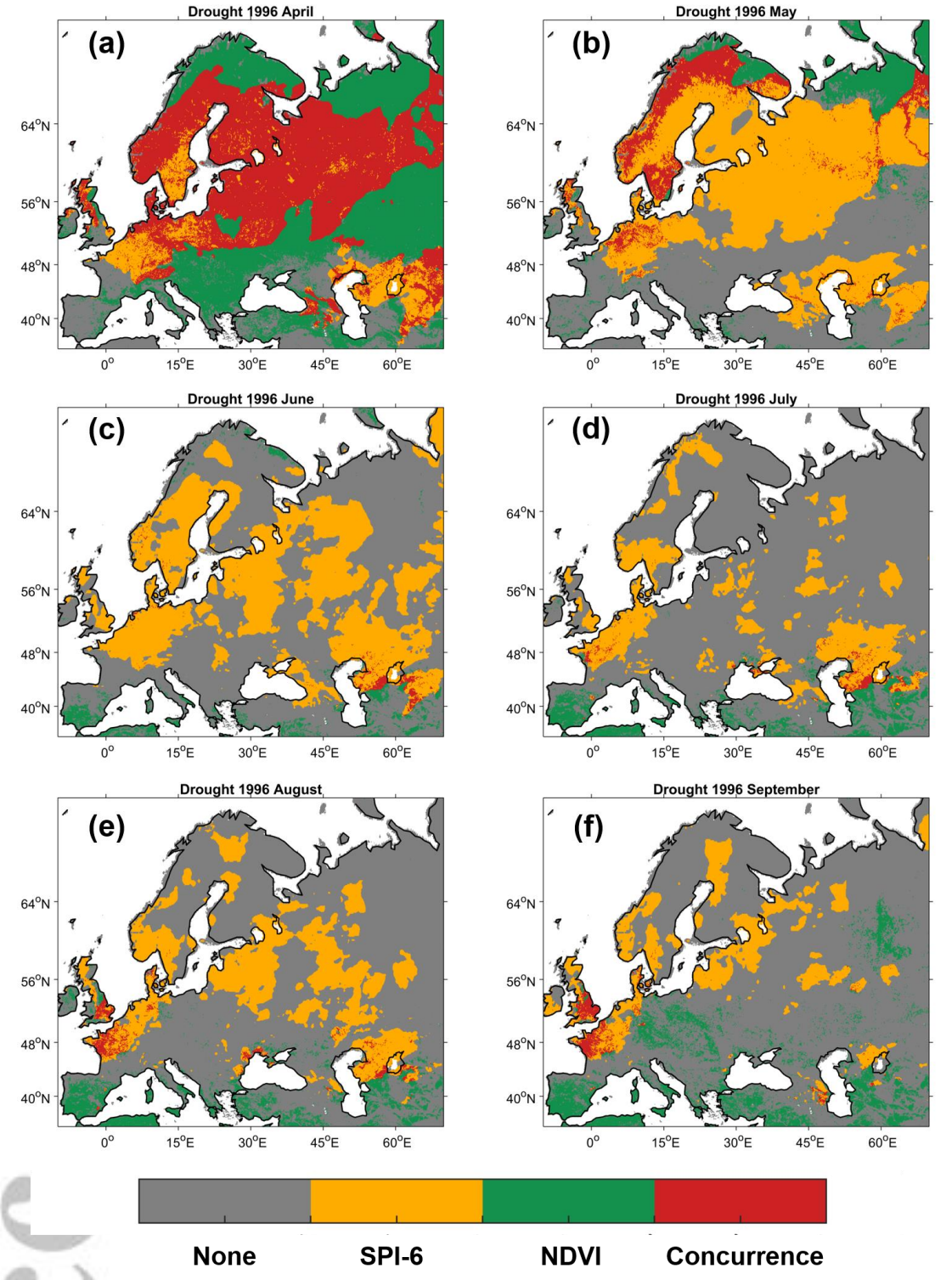

Figure 6. Concurrence of meteorological drought (SPI-6) and vegetation deficit (NDVI anomaly) during the 1996 growing season: April (a), May (b), June (c), July (d), August (e) and September (f). 'Concurrence' indicates a deficit for both SPI-6 and NDVI anomalies.

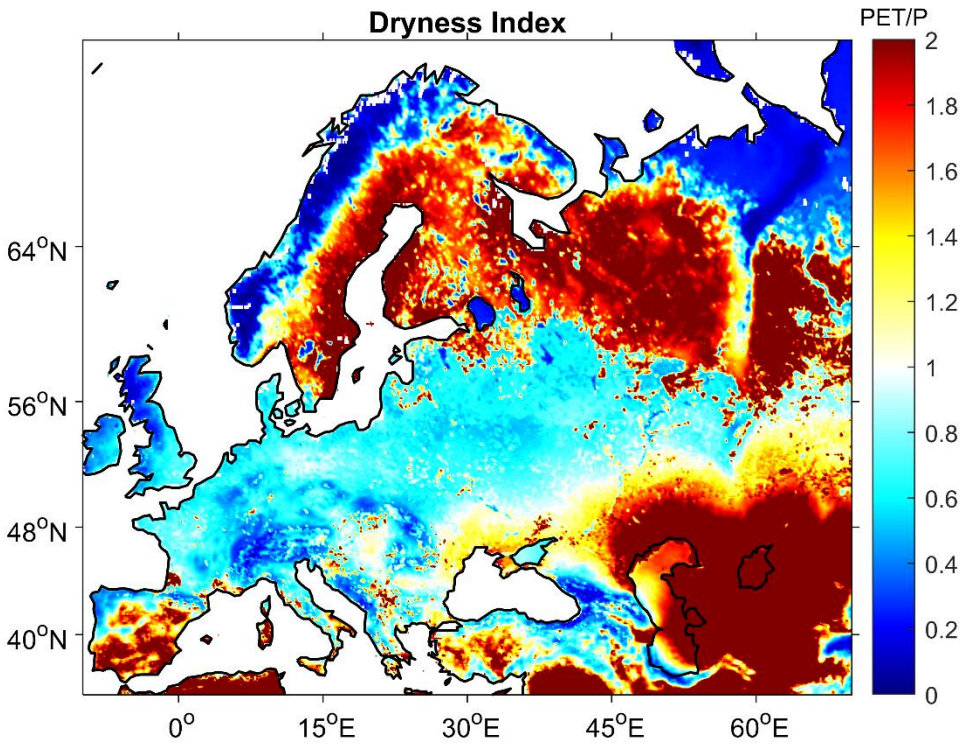

Figure 7. The dryness index pattern over WE between 1981 and 2015. Warm colors denote water-limited regions (i.e., DI > 1), and cool colors denote energy-limited regions (i.e., DI < 1).